



# Techno-economic Optimization of Isolated Hybrid Microgrids for Remote Areas Electrification: Aswan city as a Case Study

Ahmed Rashwan<sup>1</sup> · Asmaa Faragalla<sup>1</sup> · Essam M. Abo-Zahhad<sup>2,3</sup> · Adel Z. El-Dein<sup>1,4</sup> · Yuezhi Liu<sup>5</sup> · Yong Chen<sup>5</sup> · Esam H. Abdelhameed<sup>1</sup>

Received: 18 July 2023 / Accepted: 24 February 2024  
© The Author(s), under exclusive licence to Springer Nature Singapore Pte Ltd. 2024

## Abstract

Supplying electric energy in remote areas presents a significant challenge due to their relatively far distance from the main grid, low population density, high infrastructure costs, and limited resource. One promising solution to this challenge is the isolated hybrid microgrids (MGs) which can deliver reliable electricity and support economic development. The current work introduces an optimal design of isolated hybrid MGs for remote areas, whereas, a small Nubian village in Aswan, Egypt (a desert climate region) is taken as a case study. The study mainly relies on techno-economic and environmental analyses for different microgrid configurations. The analysis has been carried out utilizing Hybrid Optimization Model for Electric Renewable (HOMER Pro software) to find the least-cost design among hundreds of alternatives based on the weather conditions in this area. Recently, incorporating the renewable energy sources (RES) into local power networks is among the most prominent research areas. Although many typical components can be used to develop the required microgrid system, there are also many limitations on these components, such as resources availability and costs. Several photovoltaic (PV) /wind/diesel/storage Hybrid Energy Systems (HES) have been studied in this paper. Additionally, the effectiveness of a mechanical PV tracking system and impact of battery technologies, such as lead-acid and lithium-ion on the overall costs of the energy system has been discussed. The proposed analysis shows that the PV-wind-lithium-ion battery energy system with vertical-axis PV tracking system is the most economical option, which attains a Net Present Cost (NPC) of \$853,634.53 and a cost of energy (COE) of \$0.255 and produces acceptable environmental gas emissions of 64018.15 kg/yr. Besides, a 7 years payback of the proposed microgrid system (25-years-lifetime) has been attained.

**Keywords** Cost of Energy · HOMER software · Hybrid Energy Systems · Isolated Microgrids · Microgrid Design · Renewable energy fraction

✉ Ahmed Rashwan  
engrashwan@aswu.edu.eg

✉ Esam H. Abdelhameed  
ehhameed@energy.aswu.edu.eg

<sup>1</sup> Electrical Engineering Department, Faculty of Energy Engineering, Aswan University, Aswan 81528, Egypt

<sup>2</sup> Sustainable Energy and Power System Research Centre, Research Institute for Science and Engineering, University of Sharjah, Sharjah 27272, United Arab Emirates

<sup>3</sup> Mechanical Power Engineering Department, Faculty of Energy Engineering, Aswan University, Aswan 81528, Egypt

<sup>4</sup> Faculty of Technological Industry and Energy, Thebes Technological University, Thebes, Luxor 85863, Egypt

<sup>5</sup> School of Automation Engineering, University of Electronic Science and Technology of China, Chengdu 611731, China

## Introduction

For many centuries, fossil fuels, such as coal, oil, and gas have been used to power industrial processes and transportation systems. However, burning these fossil fuels releases large amounts of carbon dioxide into the atmosphere that trap heat from escaping back out into space, leading to increased global temperatures over time. Global carbon dioxide (CO<sub>2</sub>) emissions caused by fossil fuels are one of the primary contributors to climate change. The amount of CO<sub>2</sub> released from burning fossil fuel has risen steadily since the start of industrialization in 1750, with more than half being released after 1970 alone due to population growth and increasing demand for energy services worldwide as stated by the Intergovernmental Panel on Climate Change (IPCC), United Nations [1, 2]. In 2019 it was estimated that, around 33 billion tons of

CO<sub>2</sub> were emitted globally, with China accounting for 28%, followed by the US at 15%, India at 7%, Russia at 5%, and Japan at 4% [3]. This is a concerning trend as high levels of atmospheric CO<sub>2</sub> can lead not only to higher global temperatures but also to changes in weather patterns, which can cause extreme catastrophic weather events like floods or droughts, resulting in significant human suffering across many parts of regions on earth [4, 5]. Fortunately, many efforts and solutions have been dedicated recently for reducing the reliance on traditional sources and providing necessary energy needs with renewable energy alternatives such as solar and wind or nuclear power plants. Furthermore, improved efficiency measures through better insulation buildings or using electric vehicles instead of petrol cars offer promising potentials in that issue. These measures will help keep global temperature rises under 2°C this century if implemented quickly enough [6]. Recently, microgrids technologies have been considered an optimal solution for remote areas due to their ability to provide reliable, efficient, and clean energy [7–11]. They can generate and store electricity from various sources, such as solar, wind, hydropower, and diesel generators. Meanwhile, MGs can operate independently from the utility grid generating what so called stand-alone or isolated MGs, providing electricity when needed without relying on outside power sources. This makes them ideal for remote areas that may not have access to the utility grid or where there are frequent outages due to storms or other natural disasters [12, 13]. However, it is essential to consider any potential drawbacks of MG technologies, such as cost and/or maintenance requirements, while noting their advantages over traditional grids [14, 15]. It should also be noted that there may not be always enough RES available in some areas, which could limit the effectiveness of using hybrid MGs instead of conventional energy supplying methods like fossil fuels or nuclear power plants. Further, the environmental benefits including carbon emissions reduction comparing with the traditional grid systems are considered one of their features since they rely on renewable energy sources rather than fossil fuels. Ultimately, these features make MGs well suited for remote communities, which often have lack access to reliable electricity and have a desire for cleaner alternatives [16–18].

## Literature Review

Renewable energy resources such as solar, wind, and hydropower are essential to deliver clean energy, however, these sources are subject to intermittent nature in availability due to weather patterns or other factors [19, 20]. Commonly, incorporating RES into local conventional power networks, provides cost savings and improved reliability over time [21]. Basically, in order to maximize efficiency while minimizing costs when designing a hybrid energy microgrid system, all available resources should be taken into account. This

includes evaluating the potential output from each source based on its geographic location and weather conditions. Besides, how these resources may interact with one another in terms of load balancing or peak demand periods should be also considered. Additionally, storage capacity must be considered when determining, which combination of resources best meets a government's needs without sacrificing performance or reliability [22]. Before making any decisions about implementation strategies for a new hybrid energy microgrid system, organizations can ensure that their investments are optimized for maximum return either now or in the future through careful assessment of all the available renewable and conventional energy resources. With careful planning, this infrastructure can provide reliable, cost-effective solutions that benefit the business owners as well as the consumers.

Designing of hybrid energy systems for a remote areas is an important task that requires careful consideration and planning [23]. Developing such systems comes in three steps, the first step is to assess the energy needs of the area, including both electrical and thermal requirements. Once this data has been collected and analyzed, it can be used to identify potential sources of renewable or alternative energies, which could provide power for the region on an ongoing basis. The second step is to develop an appropriate design solution based on these findings; this could involve selecting specific technologies or combinations of the best suited for meeting local needs while providing reliable service with minimal maintenance costs over time. Finally, cost estimates should also be a factor into the design equation since installing new infrastructure requires significant upfront investments before any returns are being seen from sales revenue generated from selling the surplus electricity back onto the utility grid if applicable [24]. Many works have been found in the literature studying the optimal design for hybrid isolated MG systems. Tran et al. [25] designed a hybrid system that includes a PV system, batteries, and a diesel generator to electrify a 60 kW peak load of a remote island in Vietnam. Ozogbuda and Iqbal [26] developed a DC microgrid for a remote community of nine houses in Nigeria having a solar irradiance of 4.63 kWh/m/day. A. A. Kebede et al. [27] studied the effects of batteries and their specifications as a critical element when designing MGs for rural communities. A three-stage multi-objective mixed-integer linear programming method for optimizing the growth and operation of isolated multi-energy MGs for remote areas were proposed in [28]. Ayodele et al. [24] introduced a stand-alone microgrid composed of wind/diesel with a modular design aiming to serve residential loads and a water pumping system through a local alternating current bus. The supercapacitors energy storage is included in a standalone hybrid MG with appropriate combination supervision to balance the generation with loads proposed in [29, 30]. The combination of properly rated energy storage units and renewable

generators into isolated MGs, together with an optimal dispatching method. Authors of [31] proposed a design of an isolated MG with high penetration of RES. Virtual inertia control was introduced to improve the MG stability.

The HOMER Pro software is one of the most popular tools for sizing HES [32]. This optimization tool has the ability to identify the best size of energy systems through fast response and easy use; moreover, it can be used for sensitivity analysis to examine the effects of uncertainty or changes in input variables. Several recent studies have been conducted to verify the reliability of HOMER software for various purposes in MGs design. For example, Zhou et al. [33] used the HOMER software to design a MG system for a remote community and found that it provided accurate, reliable results. M. S. Javed et al. [34] utilized HOMER to develop a combined wind-photovoltaic hybrid system for a remote island and confirmed the satisfaction with the results. Also, Singh and Srivastava [35] used a combination of HOMER and MATLAB to design a microgrid system in a rural area and obtained efficient and reliable results. In addition, many recent studies have been conducted to analyze the performance of HOMER Pro in different scenarios. For example, in a study by Jain et al. [36], HOMER Pro was used to evaluate the economic and technical feasibility of a decentralized hybrid energy system for a remote village in India. Commonly, the hybrid energy system can significantly reduce the NPC and COE; moreover, increasing the RES penetration into the HES and reducing the Greenhouse Gas (GHG) emissions. [37].

## Motivation and Historical Background

Aswan is the sunniest city in Africa, with sunlight of 10.6 h per day i.e. almost 3863 h per year with few cloudy days. Aswan is located in the Upper Egypt (32° 53' E, longitude and 24° 5' N, latitude), it is a location where the solar power for PV technologies is available. Aswan has a subtropical desert climate and includes massive desert area indicating that it is a suitable location for efficient energy exploitation nearly through the year. Recently the Egyptian government has taken steps towards increasing renewable energy use in Aswan via establishing vast investments in solar power projects throughout the area. Benban solar park is the most notable project, which was completed in 2018, includes 41 solar power plants being developed in Benban, Aswan governorate, Egypt, by the New and Renewable Energy Authority. This project, covers over 4500 acres, making it one of the largest solar parks globally [38]. In light of Aswan's significant advancements in solar energy, highlighted by the completion of the Benban solar park, the Egyptian government is extending its commitment to renewable energy into new developmental projects. Among these initiatives is the ambitious plan to develop the Nubian villages in Wadi Karkar.

The Egyptian government plans to develop the Nubian villages in Wadi Karkar, where 8 villages will be established on an area of 400 acres, and all services will be provided there

including local power networks to meet the electrical energy requirements of approximately 2024 Nubian homes. One of these areas is governmental villages called the new Nubian city of Wadi Karkar. These villages are located in Wadi Karkar, which is 16 km from the lake Nasser in the desert.

## Research Gap

Based on previous discussion, electrification solutions for remote areas in Egypt comes in two ways, some solutions depend on PV solar production only such as Benban solar park, Aswan governorate, Egypt, whereas the other solutions relied on wind farms only to generate the power such as Ras Ghareb wind farm, Ras Ghareb, Egypt and Zafarana wind farm, Suez, Egypt. Therefore, the feasibility of integrating different renewable sources and battery system into the isolated power network based on the weather condition is expected to be most effective for these areas. In addition, this kind of research is very limited in the literature, and to the best of the authors' knowledge, few researches on optimizing both economic and environmental parameters simultaneously were conducted. Accordingly, the proposed design of hybrid solar-wind-battery for remote area with desert weather conditions is important in the current situation and for further discussion.

## Contribution of the Research

The current work makes an important contribution to addressing the challenges of electric supply in arid areas, focusing specifically on the off-grid system for desert climate remote areas, such as the new Nubian city of Karker in Aswan, Egypt. The study aims to provide reliable and cost-efficient electrification solutions in isolated areas through utilizing hybrid energy microgrid systems. One of the main contributions of this work is the thorough techno-economic and environmental analysis conducted for different microgrid architectures. By employing the HOMER optimization software, the authors explore and evaluate hundreds of alternatives and identify the least-cost design for the microgrid system. To fulfill load requirement, this comprehensive design considers net present cost (NPC), renewable energy fraction (REF), additional electrical power, cost of energy (COE), and greenhouse gas (GHG) emissions. Considering these criteria, a blueprint is formed to provide valuable insights into the most cost-effective and environmentally friendly renewable energy system for implementation. The main contributions of the study are summarized as the following:

- The study compares the utilization of different renewable energy sources, particularly solar PV systems, and small-scale wind turbines. By assessing their performance and determining the optimal utilization between the two

sources, the researchers provide practical guidance on selecting the most suitable renewable energy option for the understudy areas.

- The current study analysis helps maximizing the utilization of available resources and contributes to the overall efficiency and effectiveness of the microgrid systems.
- Highlighting the impact of solar PV mechanical tracking systems on the overall cost and performance of the energy system. By examining different tracking systems and their influence on critical factors such as NPC, REF, additional electrical power, and GHG emissions
- The study focuses on practical considerations and real-world implementation of renewable energy technologies and offers valuable information to optimize the performance of solar PV systems.
- The current work evaluates the impact of battery technologies, specifically lead-acid and lithium-ion, on the overall cost of the energy system. By comparing these technologies and their costs and performance characteristics, the study provides valuable insights into incorporating energy storage into renewable energy systems. This analysis assists in making informed choices about the most suitable battery technology based on cost and performance considerations.
- Some sensitivity parameters have been studied, such as the PV panel price, fuel price, and derating factor of the PV panels, to show the uncertainty of the proposed system.

In a nutshell, the study contributes to the existing body of knowledge. It provides a comprehensive and well-rounded analysis of the optimal design for a hybrid energy microgrid system in remote isolated areas. Its contributions to techno-economic analysis, comparison of renewable energy sources, evaluation of solar PV tracking systems, and assessment of battery technologies make it valuable for decision-makers seeking to bring reliable electricity and sustainable development to remote communities. Obviously, the current work highlights renewable energy deployment's economic and environmental benefits and offers practical guidance on system design, technology selection, and optimization.

## Article Organization

This paper has been organized as follows: in Section “[Structure of the Proposed Microgrid](#)” the structure of the proposed microgrid has been discussed including the data needed to be utilized as inputs for getting the optimal design of the microgrid in addition to the components that are suggested to be employed, Section “[Mathematical Formulation of the Problem](#)” describes the mathematical formulation of the problem. The obtained results and discussion are presented in Section “[Results and Discussions](#)”. Sensitivity analysis has been done in Section “[Sensitivity Analysis](#)” to examine the effect of the change of specific variables on the system feasibility.

Finally, this research is concluded in Section “[Conclusion and Policy Implications](#)”.

## Structure of the Proposed Microgrid

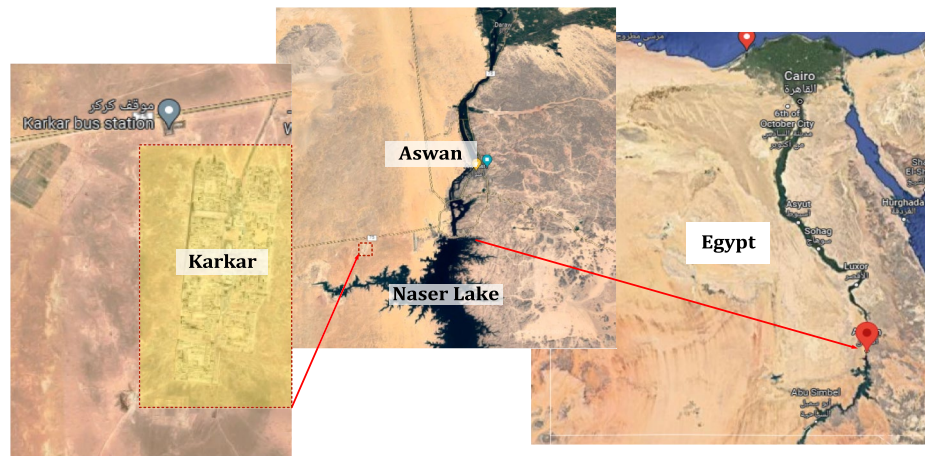
Hybrid Alternating/Direct current (AC/DC) microgrids are one of the most interesting techniques that are used in the developed distribution power networks. A typical hybrid microgrid structure is composed of AC and DC power networks. Figure 1a shows the site's location in Aswan's north (Wadi Karkar) where the proposed microgrid structure is given in Fig. 1b. As shown in the figure a hybrid AC/DC microgrid structure is proposed while the microgrid has been designed to be a self-sustaining, locally managed energy system that combines multiple sources of power generation and storage systems. It is composed of different types of distributed energy resources, i.e. renewable and non-renewable sources, such as solar PV panels, wind turbines, diesel generators, battery storage units. As depicted in the figure, an AC/DC converter works as an interfacing link between units of the hybrid AC/DC microgrid. Such converter acts as a supplier to one network and a load to the other one in islanded operation mode. Moreover, for enabling automatic operation of the isolated MG, an intelligent control system is included in the structure allowing optimal performance of the microgrid. Additionally, the proposed structure provides enhanced reliability of the power network through providing backup power in case one source fails or becomes unavailable due to weather conditions or maintenance issues.

The following sub-sections give more details for the data that has been utilized as inputs for the software aiming to obtain an optimal design i.e. the electrical loads, solar irradiation, ambient temperature, wind speed. Also, the components that are suggested to be employed in the proposed isolated microgrid such as photovoltaic modules, wind turbine, Battery Energy Storage System (BESS), DC/AC converters, and diesel generator have been discussed.

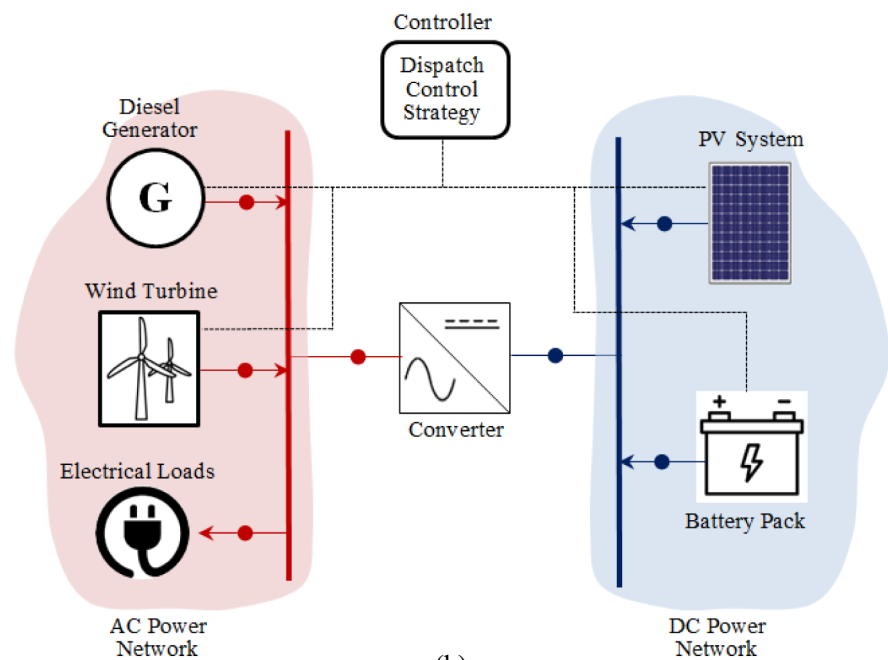
## Electrical Loads

Electrical loads in residential homes can vary greatly depending on the size and type of house, the number of occupants, and the type of the used appliances and fixtures. The typical electrical loads for a single-family home will include lighting, heating and cooling, appliances, hot water heating, and other miscellaneous items. Lighting typically accounts for the most significant portion of the electrical load, followed by heating, cooling, and appliances. Water heating and other miscellaneous items generally account for a minor part of the electrical load. In this study, for designing the understudy MG, average loads per house has been calculated for a small village composed of 10 houses with

**Fig. 1** a Site location in Aswan, b Structure of the proposed RES-based microgrid



(a)



(b)

5 occupants each. Table 1 shows the various loads existing in each house.

Figure 2 shows the daily load curve for the total residential area (small Nubian village composed of ten houses in the new Nubian city of Wadi Karkar, Aswan governorate). It is noted from the figure that the random variability in the graph represents the fluctuation in electricity usage from month to month due to changes in weather and other factors. The graph shows the peak hours of electricity usage and the average amount used during those hours. The electrical load curve for 10 houses with an average peak load of 5214 W and energy

consumption of 38346 kWh is typically bell-shaped. During peak load times, such as daytime hours when people use appliances, the electrical load curve will be higher. However, it will be lower during off-peak times, such as late-night hours (bedtime). The electrical load curve is reasonably flat over the year time, as the amount of electricity used does not fluctuate significantly as during the summer the cooling load increases, while the water heating load increases in contrast in the winter. By looking at this graph, one can determine the average electricity usage of the village and identify any potential areas of improvement.

**Table 1** Typical household electrical appliances and their operating conditions

| Item              | Power (Watts) | Quantity | Operating hours | Total load (Watt-hour) |
|-------------------|---------------|----------|-----------------|------------------------|
| Fans              | 50            | 5        | 20              | 5000                   |
| CFLs lamps        | 24            | 4        | 16              | 1536                   |
| Fluorescent Tubes | 40            | 1        | 9               | 360                    |
| TV                | 250           | 1        | 6               | 1500                   |
| Water pump        | 750           | 1        | 3               | 2250                   |
| Refrigerator      | 350           | 1        | 24              | 8400                   |
| Kettle            | 400           | 1        | 1               | 400                    |
| Air cooler        | 350           | 2        | 12              | 8400                   |
| Geyser            | 1500          | 1        | 1               | 1500                   |
| AC                | 1500          | 1        | 6               | 9000                   |
| Total             |               |          |                 | 38346                  |

### Solar Irradiation and Wind Speed

Solar irradiation curve for Aswan city is shown in Fig. 3. Aswan city receives a high amount of solar irradiation all the year. The average monthly irradiation varies between 4.57 kWh/m<sup>2</sup> in January and 7.92 kWh/m<sup>2</sup> in June, with an average daily irradiation of 6.18 kWh/m<sup>2</sup>. The total yearly irradiation in Aswan is 2,270.5 kWh/m<sup>2</sup>, with a maximum of 2,556.2 kWh/m<sup>2</sup> in June and a minimum of 1,955.6 kWh/m<sup>2</sup> in January. These data have been obtained from NASA Prediction of Worldwide Energy Resources (POWER) project. The figure also contains the monthly average wind speed data. As indicated from the figure, the wind profile in Aswan region is characterized by stable and low speeds throughout the year. The average wind speed in Aswan is around 6.0 to 7.0 m per second, with a maximum of approximately 7.06 m per second in the summer months and a minimum of about 5.94 m per second in the winter months. The wind speed

data for Aswan provide detailed information on the amount of wind energy available to the city throughout the year, which can be used in wind power generation.

### System Components

In this research, an optimized design of a hybrid microgrid has been introduced. The designed MG includes various components, which can be summarized as: diesel generators, natural gas generators, energy management system, battery management system, controllers, inverters, transformers, electrical cables, circuit breakers, and other components used to monitor and control the system. Additionally, RES like solar PV systems, wind turbines, and microturbines can be incorporated into the system. HOMER Pro software allows users to simulate different system configurations and optimize them based on user-defined objectives. Besides, the HOMER has been used to model the nominated components among the previous mentioned ones.

### Photovoltaic Modules

Generic flat-plate PV modules have been used in the proposed MG system. These modules are an effective way to generate solar power. Solar tracking PV panels are photovoltaic panels that are mounted on a tracking device to follow the sun's path throughout the day [1]. This allows the panels to capture more sunlight and generate more electricity, thus increasing the system efficiency. The tracking device can be either active or passive and ranges from a simple one-axis tracker to a more complex dual-axis tracker. The dual-axis tracker is more efficient but also more expensive. Solar tracking PV panels increase electricity production by

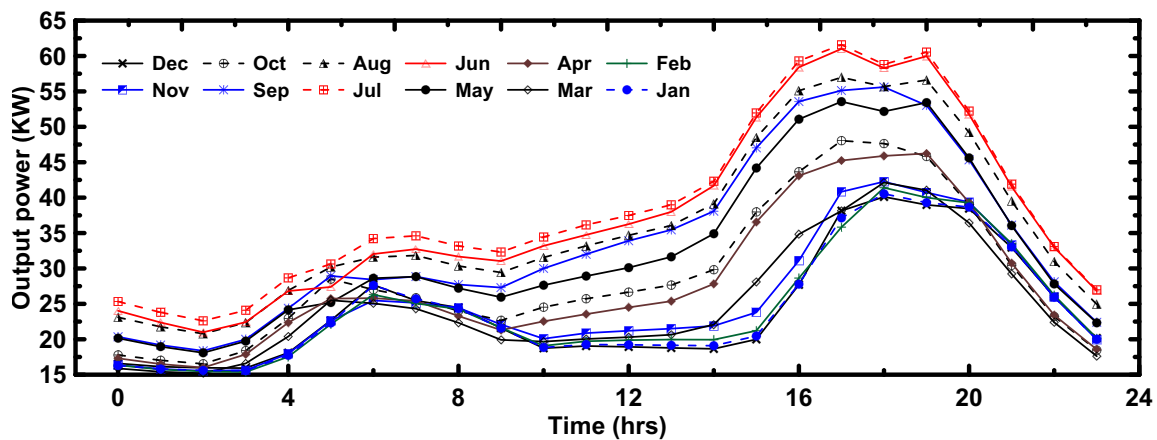


**Fig. 2** Daily load profile for the village

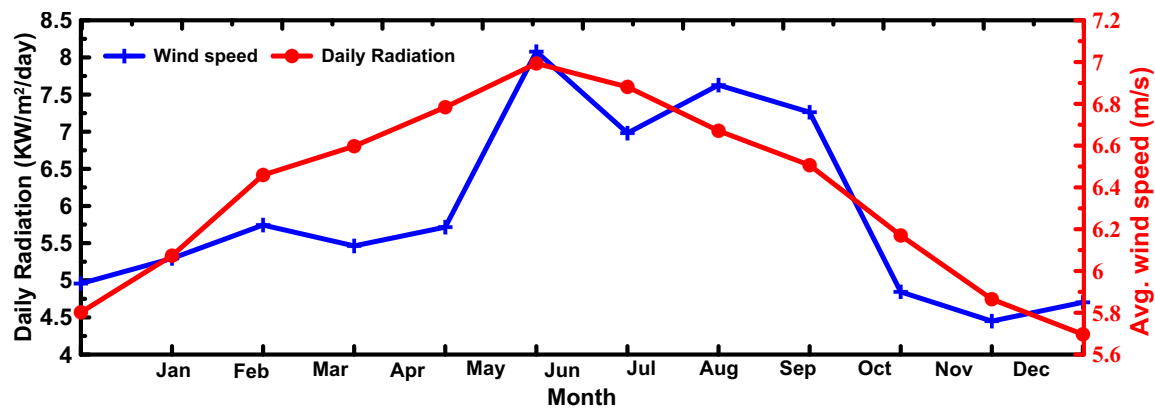


Fig. 3 Solar radiation and wind speed in Aswan city

up to 45 percent compared to stationary PV panels. The tracking systems can be classified according to horizontal and vertical tracking systems. The vertical tracking systems are typically used when space is limited to use horizontal tracking systems. (the panels need to be mounted close to the ground). On the other hand, horizontal tracking systems are typically more extensive and expensive comparing to vertical tracking systems however the panels are mounted higher off the ground and have the ability to follow the sun movements more accurately. Generally, vertical tracking systems are more economical comparing to the other tracking techniques; however, they are not as effective as the other methods for increasing the efficiency of the photovoltaic systems.

### Wind Turbine

The wind turbine depends directly on wind speed. The power output of a wind turbine is directly proportional to the cube of the wind speed, so doubling the wind speed will result in an eight-fold increase in power output. Additionally, wind turbines are designed to operate within a specific range of wind speeds, accordingly, out of this range the turbine will shut down to protect itself from damage [28].

### Battery Energy Storage System

Battery energy storage system is commonly used to store energy generated from renewable sources like solar and wind and can also be used for peak-shaving and load shifting. BESS systems are becoming increasingly popular for storing and managing energy, especially in locations where RES are heavily used. BESS is a critical component of a MG and can provide various benefits, such as increasing the power system reliability and flexibility. The most widely used types of BESS are lead-acid, lithium-ion, nickel–cadmium, and flow batteries. Lead-acid batteries are the most common and

inexpensive but have relatively low energy density and a short lifespan. Meanwhile, Lithium-ion batteries are more expensive but have higher energy density and longer lifespans. Nickel–cadmium batteries are similar to lead-acid batteries but have a shorter lifespan. Flow batteries are designed for long-term storage but are relatively expensive and have relatively low energy density. In the current work, lead-acid and lithium-ion batteries have been studied to obtain the best battery size and cost [26].

### Direct/Alternating Current (DC/AC) Converter

In a microgrid system, a DC-AC converter is an electronic device that converts direct current (DC) electricity from a renewable energy source, such as solar panels, into alternating current (AC) electricity that standard appliances can use. DC-AC converters also provide AC power from a DC power source, such as the battery, and can provide ancillary services to the grid, such as frequency regulation and power quality services. Additionally, DC-AC converters can be used to optimize the utilization of RES by reducing the amount of energy wasted due to intermittent nature of the renewable sources [13].

### Diesel Generator

Diesel generators are commonly used in MG systems as a reliable backup power source. Diesel generators convert chemical energy stored in diesel fuel into mechanical energy, which is then converted into electrical energy. Diesel generators are typically used as backup power sources in case of grid outages or when RES are unavailable. They are also used to provide additional power during peak demand periods [14].

## Mathematical Formulation of the Problem

HOMER software utilizes an objective mathematical function to find the least-cost combination of components for a MG system. The main objective is to minimize the cost of energy while also accounting for the cost of capital and other system components. The total NPC can be defined as the sum of all of the costs associated with a MG system over its lifetime, taking into account the cost of capital and system components. This includes the cost of the power sources, energy storage systems, energy management systems, battery management systems, MG controllers, programmable logic controllers, and any other costs associated with the system. The total NPC is used to compare and evaluate different MG systems and to identify the least-cost combination of components for a particular system.

$$\sum (\text{Discounted Cash Flows}) = \text{Sum of all the discounted cash flows} \quad (2)$$

$$\text{Initial Investment} = \text{The initial investment made in the project or investment} \quad (3)$$

The formula for calculating the discounted cash flow for a particular cash flow is:

$$\text{Discounted Cash Flow} = \frac{\text{cash flow}}{(1+r)^t} \quad (4)$$

where the *cashflow* is the amount of cash flow for a particular period, *r* is the discount rate, and *t* is the period number.

The cost of energy is another factor for the optimization algorithm in HOMER software. It is a measure of the average cost of electricity generation over the life of a project. It considers all the materials, labor, and other expenses associated with operating the project, as well as any expected disposal costs. It is calculated by dividing the total present value of all the costs related to the project by the total energy generated over its lifetime. The COE is an essential metric for evaluating the economic feasibility of a project and is often used to compare different sources of energy.

The formula for calculating the COE is as follows:

$$\text{COE} = \frac{\text{Total Cost of Production} - \text{Thermal Load Cost}}{\text{Total Energy Produced}} \quad (5)$$

This formula considers the total cost of producing electricity, including purchasing, installing, operating, and maintaining the project or investment, and divides it by the total energy produced. This provides the cost of electricity that is produced by the project or investment. The overall flowchart of the strategies involved in the proposed design utilizing HOMER software is shown in Fig. 4.

The steps to calculate the NPC are as follows:

1. Identify all of the costs associated with the project.
2. Estimate the cash flow for each cost item.
3. Discount each cash flow to the same base date.
4. Sum up all the discounted cash flows.
5. Subtract the initial investment amount.
6. Calculate the net present value.

So, the formula for calculating the NPC is:

$$\text{NPC} = \sum (\text{Discounted Cash Flows}) - \text{Initial Investment} \quad (1)$$

where:

## Results and Discussions

The input parameters and costs of PV, wind turbine, diesel generator, battery, and inverter are shown in Table 2. The technical parameters and price of the components have been taken from different references and some commercial websites. The inputs to HOMER software are essential for accurately modeling the system and predicting its performance. Inputs include the size and type of components, their costs, power output, efficiency, and other technical parameters. Additionally, the inputs include data about the local environment, such as solar irradiance, wind speed, and temperature. All this data is essential for ensuring appropriate system design.

### Impact of the Wind Turbine Size on the Proposed Microgrid

The size of the wind turbines used in a MG system significantly affects the overall system's cost. HOMER can be used to simulate different scenarios with various wind turbine sizes and calculate their impact on the local environment, such as their effect on the cost of energy production. HOMER can also be used to optimize the layout and design of wind farms to maximize efficiency. By optimizing the MG system, the cost of energy production can be reduced significantly, making wind energy more affordable and accessible to more people. Tables 3, 4, 5 and 6 show the results of four scenarios based on the previously mentioned input



**Fig. 4** Flowchart of the optimization process using HOMER Pro software

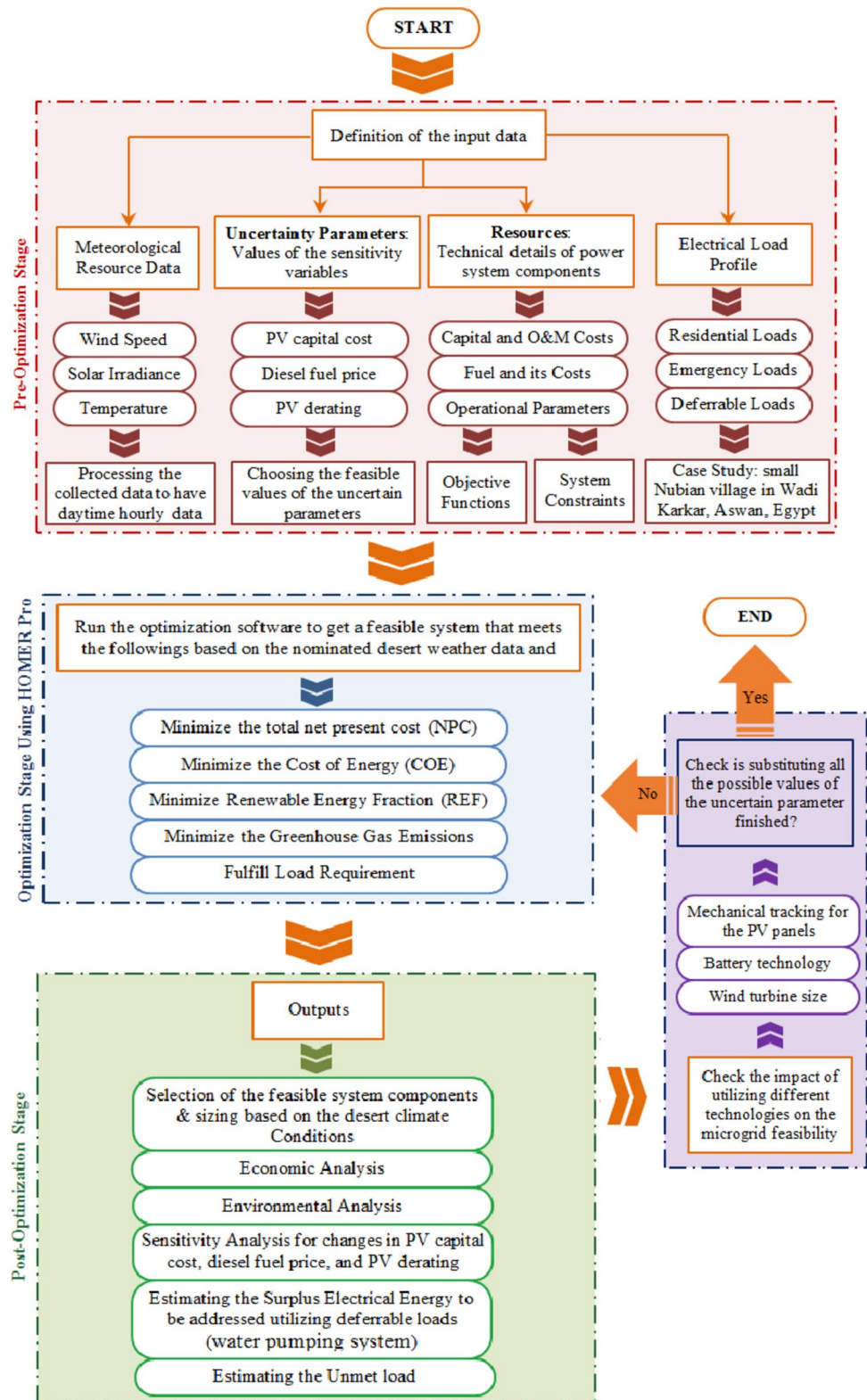


**Table 2** Specifications and cost of the components used to configure the microgrid

| Item                           | Description                               | Specification                |
|--------------------------------|---|------------------------------|
| 1. PV system                   | Type                                      | Flat Canadian Solar MaxPower |
|                                | Nominal power                             | 0.325 KW                     |
|                                | Tracking system                           | Fixed/ Multi                 |
|                                | Efficiency at the standard test condition | 16.94%                       |
|                                | Temperature coefficient                   | 0.48%/°C                     |
|                                | Nominal operating cell temperature        | 47° C                        |
|                                | Derating factor                           | 88%                          |
|                                | Ground reflection                         | 20%                          |
|                                | Capital cost                              | 1000 \$/KW                   |
|                                | Operating and maintenance cost            | 5 \$/year                    |
|                                | Cost of replacement                       | 1000 \$/KW                   |
|                                | Lifetime                                  | 25 years                     |
|                                | 2. Wind turbine                           | Type                         |
| Hub Height                     |   | 10 m                         |
| Cut-in wind speed:             |   | 1.5 m/s                      |
| Number of blades               |   | 3                            |
| Material                       |   | aluminum alloy               |
| Generator type                 |   | synchronous permanent        |
| Capital cost                   |   | 5000 \$                      |
| Cost of replacement            |   | 5000 \$                      |
| Operating and maintenance cost |   | 200 \$/year                  |
| Lifetime                       |   | 20 years                     |
| 3. Diesel generator            | Capital cost                              | 2200 \$                      |
|                                | Operating and maintenance cost            | 1 \$/hour                    |
|                                | Replacement cost                          | 2200 \$                      |
| 4. Batteries<br>(Lead acid)    | Lifetime                                  | 15000 h                      |
|                                | Nominal capacity                          | 83.4 Ah                      |
|                                | Capital cost                              | 300 \$                       |
|                                | Operating and maintenance cost            | \$10/year                    |
| 5. Batteries<br>(Lithium-Ion)  | Replacement cost                          | 300 \$                       |
|                                | Lifetime throughout                       | 4 years                      |
|                                | Capital cost                              | 2000 \$                      |
|                                | Lifetime throughout                       | 10 years                     |
| 6. Converter                   | Nominal capacity                          | 100 Ah                       |
|                                | Capital cost                              | \$550/kW                     |
|                                | Operating and maintenance cost            | \$ 5/kW/year                 |
|                                | Replacement                               | \$ 450/kW                    |
|                                | Lifetime                                  | 10 years                     |

data and utilizing different sizes of wind turbines. Table 3 illustrates the results of the first scenario in which a wind turbine with size of 1.5 kW is utilized. The optimal architecture is obtained with NPC of \$1.19 M and COE of \$0.354, whereas the CO<sub>2</sub> emission in this scenario is 90,397 kg/year. It is observed from the table that the optimal system does not include a wind turbine. The system that contains wind turbines came in second level with a slight increase in COE price. In the second scenario the size of the wind turbine has been increased to 3.3 kW, the optimal results are shown in Table 4. The optimal system in this scenario includes

14 wind turbines with a total NPC of \$ 1.01 M, which is less than in case of 1.0 kW wind turbine scenario. Also, the CO<sub>2</sub> emission is improved to a value of 67.796 kg/year compared to 90,397 kg/year in the first scenario. The third scenario has been tested by increasing the wind size to 5.1 kW, the obtained results are shown in Table 5. A reduction of the total NPC has been obtained. The NPC and COE, in this case, are \$ 1.0 M and \$ 0.30, respectively. In the final scenario, the system has been simulated without utilizing any wind turbine, and the results are shown in Table 6. It is observed that the obtained NPC and COE for such a scenario

**Table 3** Best microgrid configurations based on 1.5 kW wind turbine scenario

| Design # | PV (kW) | Wind turbine (kW) | Diesel (kW) | BESS (kWh) | Inverter (kW) | Dispatch Strategy | Total NPC (\$) | Energy cost (\$/kWh) | Operating cost (\$/yr) | Initial capital (\$) | Fuel cost (\$/yr) | CO <sub>2</sub> (kg/yr) |
|----------|---------|-------------------|-------------|------------|---------------|-------------------|----------------|----------------------|------------------------|----------------------|-------------------|-------------------------|
| 1        | 231.82  | —                 | 20          | 466        | 64.574        | LF                | 1187084.0      | 0.4                  | 60411.9                | 406107.3             | 17279.9           | 90396.73                |
| 2        | 250.62  | 2 × 1.5           | 20          | 446        | 61.748        | LF                | 1194747.0      | 0.4                  | 59350.0                | 427498.4             | 17039.9           | 89141.45                |
| 3        | —       | 162 × 1.5         | 20          | 862        | 74.306        | CC                | 2852403.0      | 0.9                  | 134940.9               | 1107953.0            | 13243.4           | 69280.45                |

**Table 4** Best microgrid configurations based on 3.3 kW wind turbine scenario

| Design # | PV (kW) | Wind turbine (kW) | Diesel (kW) | BESS (kWh) | Inverter (kW) | Dispatch Strategy | Total NPC (\$) | Energy cost (\$/kWh) | Operating cost (\$/yr) | Initial capital (\$) | Fuel cost (\$/yr) | CO <sub>2</sub> (kg/yr) |
|----------|---------|-------------------|-------------|------------|---------------|-------------------|----------------|----------------------|------------------------|----------------------|-------------------|-------------------------|
| 1        | 130.29  | 14 × 3.3          | 20          | 358        | 51.55326      | LF                | 1013847        | 0.302711             | 50294.59               | 363663.3             | 12959.58          | 67795.86                |
| 2        | 213.49  | —                 | 20          | 453        | 59.33007      | CC                | 1198752        | 0.357882             | 63237.05               | 381253.5             | 20421.02          | 106829.2                |
| 3        | —       | 39 × 3.3          | 20          | 822        | 52.99719      | CC                | 1745383        | 0.521222             | 92599.69               | 548298.6             | 14556.07          | 76147.63                |

**Table 5** Best microgrid configurations based on 5.1 kW wind turbine scenario

| Design # | PV (kW) | Wind turbine (kW) | Diesel (kW) | BESS (kWh) | Inverter (kW) | Dispatch Strategy | Total NPC (\$) | Energy cost (\$/kWh) | Operating cost (\$/yr) | Initial capital (\$) | Fuel cost (\$/yr) | CO <sub>2</sub> (kg/yr) |
|----------|---------|-------------------|-------------|------------|---------------|-------------------|----------------|----------------------|------------------------|----------------------|-------------------|-------------------------|
| 1        | 125.498 | 9 × 5.1           | 20          | 360        | 56.45577      | LF                | 1004137        | 0.299827             | 50296.68               | 353925.6             | 13583.98          | 71062.31                |
| 2        | 213.488 | —                 | 20          | 453        | 59.33007      | CC                | 1198752        | 0.357882             | 63237.05               | 381253.5             | 20421.02          | 106829.2                |
| 3        | —       | 33 × 5.1          | 20          | 589        | 53.80615      | CC                | 1481342        | 0.442356             | 73141.59               | 535803.1             | 13098.56          | 68522.94                |

**Table 6** Best microgrid configurations based on no wind turbine used scenario

| Design # | PV (kW) | Diesel (kW) | BESS (kWh) | Inverter (kW) | Dispatch Strategy | Total NPC (\$) | Energy cost (\$/kWh) | Operating cost (\$/yr) | Initial capital (\$) | Fuel cost (\$/yr) | CO <sub>2</sub> (kg/yr) |
|----------|---------|-------------|------------|---------------|-------------------|----------------|----------------------|------------------------|----------------------|-------------------|-------------------------|
| 1        | 199.63  | 20          | 547        | 54.805        | LF                | 1004092.0      | 0.2998               | 47244.89               | 393332.5             | 17688.01          | 92531.88                |

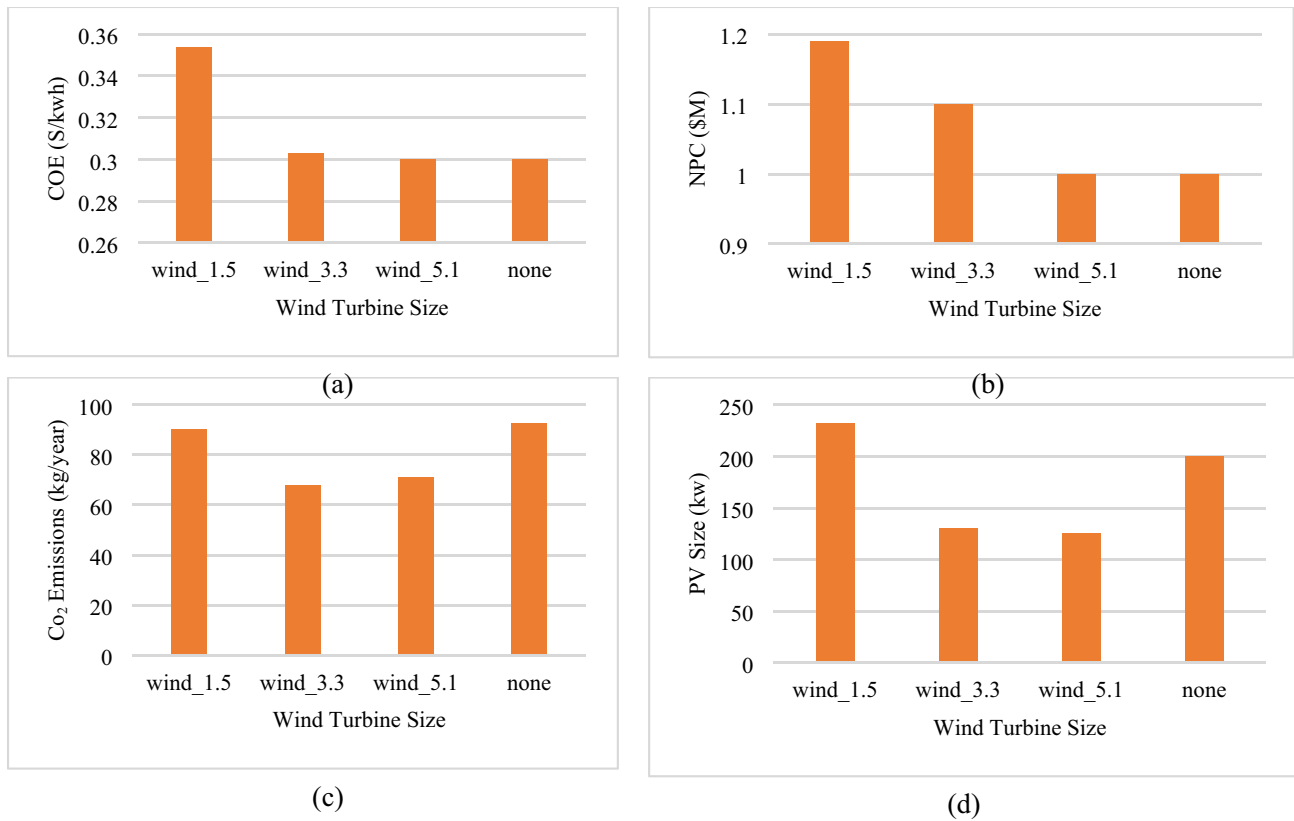


**Fig. 5** Comparison between different wind turbine sizes with respect to: **a** COE, **b** NPC, **c** CO<sub>2</sub> Emissions, and **(d)** PV size

are \$ 1.0 M and \$ 0.30, respectively, which are the same values using a wind turbine. The PV size, in this case, is 200 kW, while with the wind turbine in scenario 3, and the PV size is 125 kW. So, the operator can select the optimal design between the two scenarios according to the available components and land space.

Figure 5a-d show the visual analysis of the data in previous tables to get a better view of the optimal design. The figures compare each scenario's NPC, COE, and CO<sub>2</sub> emissions. The PV size is also shown, as it is a key factor in selecting the optimal design. It is observed that the small wind turbine case (1.5 kW) is the worst scenario as this scenario resulting in high NPC, COE, and CO<sub>2</sub> emissions. Due to there are largely undeveloped areas in Aswan region, the available land for constructing PV systems is considered a limiting factor. Accordingly, and based on Fig. 5 (i.e. from the COE, NPC, and CO<sub>2</sub> emissions viewpoints), the first solution in the third scenario is considered the optimal choice for designing an isolated microgrid for the understudy Nubian village in Wadi Karkar.

### Effect of the Mechanical Tracking for the PV Panels

The cost of a PV system with mechanical tracking is generally higher than a PV system without tracking. A single-axis

tracking system may cost up to \$1,300 per kW, while a dual-axis tracking system may cost up to \$1,500 per kW. This cost difference is mainly due to the additional components needed for the tracking system, such as motors and sensors, in addition to the extra energy and maintenance costs associated with the dual-axis tracking system. However, the increased cost is offset by the increased efficiency of the tracking system, as it can increase the power output of a solar panel by up to 40%. The system has been simulated under five different mechanical tracking techniques (i.e. vertical-axis continuous (VA cont.) tracking, horizontal-axis continuous (HA cont.) tracking, dual-axis continuous (2A cont.) tracking, horizontal-axis daily (HA daily) tracking, horizontal-axis weekly (HA weekly) tracking, and horizontal-axis monthly (HA monthly) tracking) where the obtained results are presented in Table 7, 8, 9, 10, 11, 12 and Fig. 6.

It is clear from Fig. 6 that, when compared to other tracking techniques, the vertical-axis tracking technique generally has the lowest value in terms of NPC and the COE with values of \$ 913,216.0 and \$ 0.274, respectively, indicating that the vertical-axis tracking technique is the best choice for designing the isolated hybrid microgrid in the understudy area comparing to the best configuration without PV tracking system, the best solution with vertical-axis tracking technique allows lower NPC and CO<sub>2</sub> emissions with values

**Table 7** Best microgrid configurations based on horizontal-axis monthly tracking technique

| Design # | PV (kW) | Wind turbine (kW) | Diesel (kW) | BESS (kWh) | Inverter (kW) | Dispatch Strategy | Total NPC (\$) | Energy cost (\$/kWh) | Operating cost (\$/yr) | Initial capital (\$) | Fuel cost (\$/yr) | CO <sub>2</sub> (kg/yr) |
|----------|---------|-------------------|-------------|------------|---------------|-------------------|----------------|----------------------|------------------------|----------------------|-------------------|-------------------------|
| 1        | 114.256 | 11 × 5.1          | 20          | 335        | 51.763        | LF                | 991167.8       | 0.296                | 47610.0                | 375688.8             | 12588.26          | 65853.35                |
| 2        | 203.038 | —                 | 20          | 431        | 70.595        | CC                | 1206769.0      | 0.360                | 61599.3                | 410443.5             | 20175.03          | 105542.3                |
| 3        | —       | 33 × 5.1          | 20          | 589        | 53.806        | CC                | 1481342.0      | 0.442                | 73141.59               | 535803.1             | 13098.56          | 68522.94                |

**Table 8** Best microgrid configurations based on horizontal-axis weekly tracking technique

| Design # | PV (kW) | Wind turbine (kW) | Diesel (kW) | BESS (kWh) | Inverter (kW) | Dispatch Strategy | Total NPC (\$) | Energy cost (\$/kWh) | Operating cost (\$/yr) | Initial capital (\$) | Fuel cost (\$/yr) | CO <sub>2</sub> (kg/yr) |
|----------|---------|-------------------|-------------|------------|---------------|-------------------|----------------|----------------------|------------------------|----------------------|-------------------|-------------------------|
| 1        | 113.628 | 11 × 5.1          | 20          | 334        | 52.403        | LF                | 989649.3       | 0.295                | 47549.27               | 374955.3             | 12584.11          | 65831.67                |
| 2        | 203.038 | —                 | 20          | 431        | 70.595        | CC                | 1206554.0      | 0.360                | 61582.66               | 410443.5             | 20162.99          | 105479.3                |
| 3        | —       | 33 × 5.1          | 20          | 589        | 53.806        | CC                | 1481342.0      | 0.442                | 73141.59               | 535803.1             | 13098.56          | 68522.94                |

**Table 9** Best microgrid configurations based on horizontal-axis daily tracking technique

| Design # | PV (kW) | Wind turbine (kW) | Diesel (kW) | BESS (kWh) | Inverter (kW) | Dispatch Strategy | Total NPC (\$) | Energy cost (\$/kWh) | Operating cost (\$/yr) | Initial capital (\$) | Fuel cost (\$/yr) | CO <sub>2</sub> (kg/yr) |
|----------|---------|-------------------|-------------|------------|---------------|-------------------|----------------|----------------------|------------------------|----------------------|-------------------|-------------------------|
| 1        | 113.628 | 11 × 5.1          | 20          | 334        | 52.403        | LF                | 989682.6       | 0.296                | 47551.84               | 374955.3             | 12585.53          | 65839.1                 |
| 2        | 201.009 | —                 | 20          | 433        | 68.819        | CC                | 1205459.0      | 0.360                | 61708.63               | 407719.7             | 20200.37          | 105674.9                |
| 3        | —       | 33 × 5.1          | 20          | 589        | 53.806        | CC                | 1481342.0      | 0.442                | 73141.59               | 535803.1             | 13098.56          | 68522.94                |

**Table 10** Best microgrid configurations based on horizontal-axis continuous tracking technique

| Design # | PV (kW) | Wind turbine (kW) | Diesel (kW) | BESS (kWh) | Inverter (kW) | Dispatch Strategy | Total NPC (\$) | Energy cost (\$/kWh) | Operating cost (\$/yr) | Initial capital (\$) | Fuel cost (\$/yr) | CO <sub>2</sub> (kg/yr) |
|----------|---------|-------------------|-------------|------------|---------------|-------------------|----------------|----------------------|------------------------|----------------------|-------------------|-------------------------|
| 1        | 113.683 | 10 × 5.1          | 20          | 311        | 51.954        | LF                | 949991.8       | 0.284                | 45801.21               | 357895.9             | 12789.87          | 66908.07                |
| 2        | 221.580 | —                 | 20          | 410        | 67.538        | LF                | 1143693.0      | 0.341                | 55604.52               | 424864.5             | 16708.77          | 87409.14                |
| 3        | —       | 33 × 5.1          | 20          | 589        | 53.806        | CC                | 1481342.0      | 0.442                | 73141.59               | 535803.1             | 13098.56          | 68522.94                |

**Table 11** Best microgrid configurations based on vertical-axis continuous tracking technique

| Design # | PV (kW)  | Wind turbine (kW) | Diesel (kW) | BESS (kWh) | Inverter (kW) | Dispatch Strategy | Total NPC (\$) | Energy cost (\$/kWh) | Operating cost (\$/yr) | Initial capital (\$) | Fuel cost (\$/yr) | CO <sub>2</sub> (kg/yr) |
|----------|----------|-------------------|-------------|------------|---------------|-------------------|----------------|----------------------|------------------------|----------------------|-------------------|-------------------------|
| 1        | 97.35124 | 11 × 5.1          | 20          | 296        | 52.01371      | LF                | 913215.6       | 0.272676             | 44044.6                | 343828.3             | 12100.15          | 63299.93                |
| 2        | 216.2046 | —                 | 20          | 398        | 60.4649       | LF                | 1111467.0      | 0.331875             | 54162.7                | 411278               | 16427.41          | 85937.26                |
| 3        | —        | 33 × 5.1          | 20          | 589        | 53.80615      | CC                | 1481342        | 0.442356             | 73141.59               | 535803.1             | 13098.56          | 68522.94                |

**Table 12** Best microgrid configurations based on dual-axis continuous tracking technique

| Design # | PV (kW) | Wind turbine (kW) | Diesel (kW) | BESS (kWh) | Inverter (kW) | Dispatch Strategy | Total NPC (\$) | Energy cost (\$/kWh) | Operating cost (\$/yr) | Initial capital (\$) | Fuel cost (\$/yr) | CO <sub>2</sub> (kg/yr) |
|----------|---------|-------------------|-------------|------------|---------------|-------------------|----------------|----------------------|------------------------|----------------------|-------------------|-------------------------|
| 1        | 82.967  | 12 × 5.1          | 20          | 290        | 51.827        | LF                | 917412.8       | 0.274                | 43793.89               | 351266.6             | 11726.99          | 61347.76                |
| 2        | 174.513 | —                 | 20          | 413        | 55.916        | CC                | 1163743.0      | 0.348                | 59204.36               | 398377.2             | 19011.29          | 99454.38                |
| 3        | —       | 33 × 5.1          | 20          | 589        | 53.806        | CC                | 1481342.0      | 0.442                | 73141.59               | 535803.1             | 13098.56          | 68522.94                |

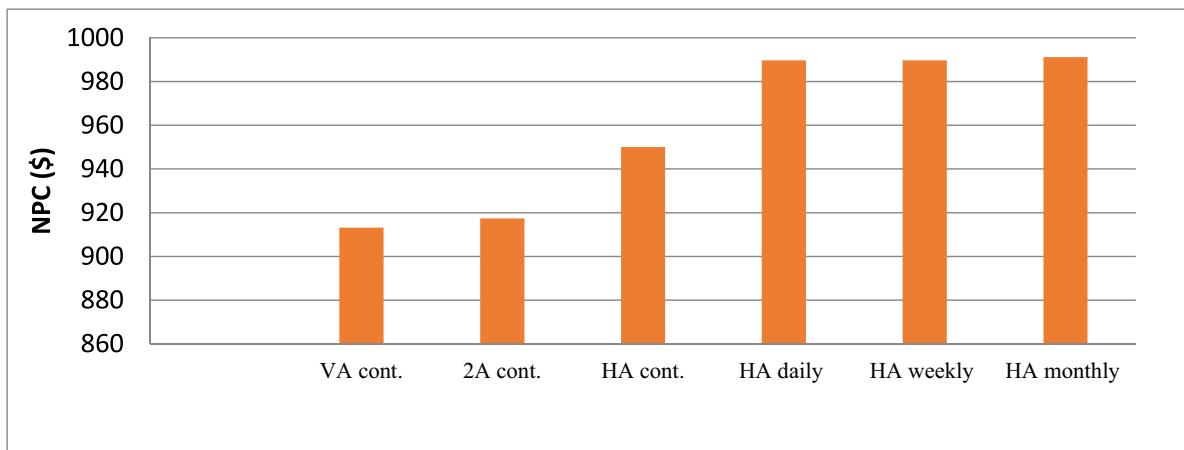


**Fig. 6** Comparison based on different tracking systems

of \$ 913,216.0 and 61347.76 kg/yr, respectively, where these values are \$ 1004137, and 71062.31 kg/yr, respectively.

### Effect of Adding Lithium-ion battery

Lithium-ion batteries generally cost more than lead-acid batteries but are also much more efficient. Lead-acid batteries are cheaper to produce, but they are also less efficient and have shorter lifespans than lithium-ion batteries. Lithium-ion batteries are much more efficient than lead-acid batteries, meaning they can store more energy for the same volume. Lithium-ion batteries are also more efficient in charge and discharge, meaning they can be charged and discharged more quickly than lead-acid batteries. Table 13 present the analysis of using both battery types in the proposed MG system. It is clear that adding a lithium-ion battery to an electrical MG system can significantly impact the NPC and COE values. The study has shown that adding a lithium-ion battery to a MG system can reduce the NPC and COE to \$853,635 and \$0.255, respectively. This is a significant reduction as it can help to lower energy costs and make the system more efficient and stable. The lithium-ion battery can provide energy storage and can be used to store energy generated from renewable sources like solar and wind, reducing the need for traditional sources of energy. The lithium-ion battery can also provide fast and reliable power when needed, helping stabilize the system and reduce the need for backup generators.

Table 14 shows the costs of individual components in terms of capital cost, replacement cost, operations and maintenance cost, fuel cost, salvage cost, and the total cost. The capital cost is the most significant project cost and includes the cost of purchasing and installing the component. Replacement costs cover the costs associated with replacing a component due to wear and tear. Operations

and maintenance cost is related to the component cost over its lifetime. Fuel costs are the costs of purchasing fuel to power the component. Salvage costs are the costs associated with salvaging the component at the end of its useful life. Finally, the total cost is the sum of all the individual costs associated with the component. Figure 7 shows a graphical comparison of the cost of different system components. It is clear from the figure that the batteries have the highest cost in the system, followed by PV panels and wind turbines. The cost of the batteries is significantly higher than the other components, likely due to their high energy storage capacity. The cost of PV panels and wind turbines are much lower, probably due to their relatively simple design. This graphical comparison allows for a quick and easy comparison of the relative costs of the different components and provides valuable insight into the costs associated with the system.

Figure 8 shows generated energy from the available power sources. The proposed MG system has been designed to deliver a 709 kWh/day and provide a peak power of 68 kW. To meet this demand, the following generation sources of energy have been utilized: solar system, wind turbines, diesel generators, and battery energy storage system. Depending on the availability of these sources, the MG system may draw from all of the sources or a combination of them to meet the electrical load. The cost of the individual components, including capital cost, replacement cost, Operations and maintenance cost, fuel cost, salvage cost, and total cost, should be considered to determine the most cost-effective system that meets the electrical load.

Figure 9 shows the daily load demand along with the power generated from the BESS or from the different utilized power systems whether conventional or renewable. The figure illustrates how the battery can store renewable energy during the day and then provide energy throughout the night,

**Table 13** Best microgrid configurations based on Lithium-ion batteries utilization

| Design # | PV (kW)  | Wind turbine (kW) | Diesel (kW) | BESS (kW/h) Lead-acid | BESS (kW/h) Lithium-ion | Inverter (kW) | Dispatch Strategy | Total NPC (\$) | Energy cost (\$/kWh) | Operating cost (\$/yr.) | Initial capital (\$) | Fuel cost (\$/yr.) | CO <sub>2</sub> (kg/yr.) |
|----------|----------|-------------------|-------------|-----------------------|-------------------------|---------------|-------------------|----------------|----------------------|-------------------------|----------------------|--------------------|--------------------------|
| 1        | 85.62402 | 11                | 20          | —                     | 151                     | 63.46887      | LF                | 853634.6       | 0.254891             | 23589.32                | 548683.3             | 12237.45           | 64018.15                 |
| 2        | 97.35124 | 11                | 20          | 296                   | —                       | 52.01371      | LF                | 913215.6       | 0.272676             | 44044.6                 | 343828.3             | 12100.15           | 63299.93                 |
| 3        | 205.5573 | —                 | 20          | —                     | 195                     | 56.52797      | LF                | 1098093        | 0.32787              | 33336.69                | 667132.8             | 16604.81           | 86865.27                 |

allowing for more efficient and reliable use of renewable energy. This scenario is considered a typical example of how battery energy storage systems can help enhancing renewable energy use in the power networks (Fig. 10).

Renewable energy penetration is the percentage of total energy generated from renewable sources with respect to the loads such as wind, solar, geothermal, and hydro. Increasing renewable penetration is an important step in transitioning away from fossil fuels and reducing greenhouse gas emissions. Figure 11 depicts the monthly average penetration of the proposed system. The maximum penetration is occurred during March with a value of 749 kW. The proposed configuration reduces the operating costs to \$23,589/yr. The payback, the Internal Rate of Return (IRR), and the Return on Investment (ROI) are important financial metrics, which are the amount of time it takes to recover an investment's initial cost, an estimation of the profitability of potential investments, and the yearly cost savings relative to the initial investment, respectively. The proposed isolated microgrid is designed for 25-years-lifetime, as an investment it has a payback of 7 years, an IRR of 8.47%, and ROI of 6.38%.

The design of isolated microgrids encounters numerous challenges, including managing the surplus electrical energy. One potential solution to address this issue is the use of deferrable loads. In this paper, we propose a water pumping system as a deferrable load to reduce the excess of the electrical energy. The system is designed with a load of 200 kW/day and a peak load of 20 kW, assuming an equal distribution of the load throughout the year. Our results show that the use of the deferrable load reduces the excess energy from 30 to 21%. However, it is important to note that the energy management procedure used in this study does not entirely eliminate excess energy. Other loads, such as thermal loads, can be added, but require careful study to ensure optimal management. Overall, the use of deferrable loads offers a promising solution to reduce the surplus electrical energy in isolated microgrids.

## Sensitivity Analysis

In this study, a sensitivity analysis was conducted using the HOMER software to investigate the impact of three key factors on the performance and economics of a hybrid renewable energy system. Specifically, the sensitivity of the system to changes in PV capital cost, diesel fuel price, and PV derating has been evaluated. The results showed that when the PV capital and replacement costs decreased, the installed PV capacity increased, while the total net present cost (NPC) decreased. For instance, when the cost ratio of the PV decreased to 0.8 of its value, the NPC decreased from \$853,634 to \$833,059.4. On the other hand, increasing the diesel fuel price led to an increased



**Table 14** Comparison of the cost of the best system components (with Lithium-ion batteries)

| Component    | Capital (\$) | Replacement (\$) | O&M (\$)     | Fuel (\$) | Salvage (\$) | Total (\$)   |
|--------------|--------------|------------------|--------------|-----------|--------------|--------------|
| Diesel       | \$2,200.00   | \$6,846.61       | \$54,114.58  | \$158.199 | -\$12.30     | \$221,348.68 |
| Wind Turbine | \$110,000.00 | \$35,068.81      | \$28,440.54  | \$0.0     | -\$19,763.52 | \$153,745.82 |
| PV           | \$102,748.83 | \$12821.24       | \$5,534.53   |           | \$0.00       | \$108,283.36 |
| Inverter     | \$31,734.44  | \$16,821.24      | \$12,307.42  | \$0.00    | -\$2,280.67  | \$58,582.43  |
| Battery      | \$302,000.00 | \$22821.24       | \$19,520.55  | \$0.00    | -\$9,846.31  | \$311,674.24 |
| Total System | \$548,683.27 | \$58,736.65      | \$119,917.62 | \$158.199 | -\$31,902.80 | \$853,634.53 |

**Fig. 7** Costs of individual components

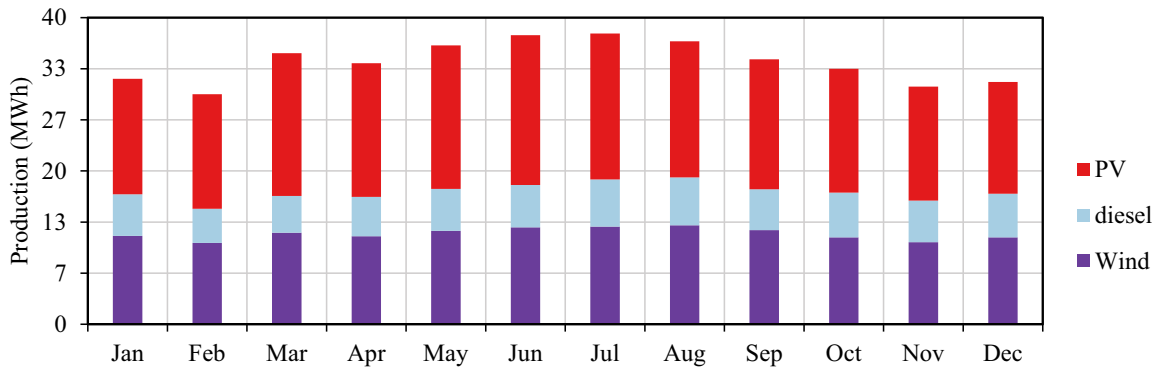
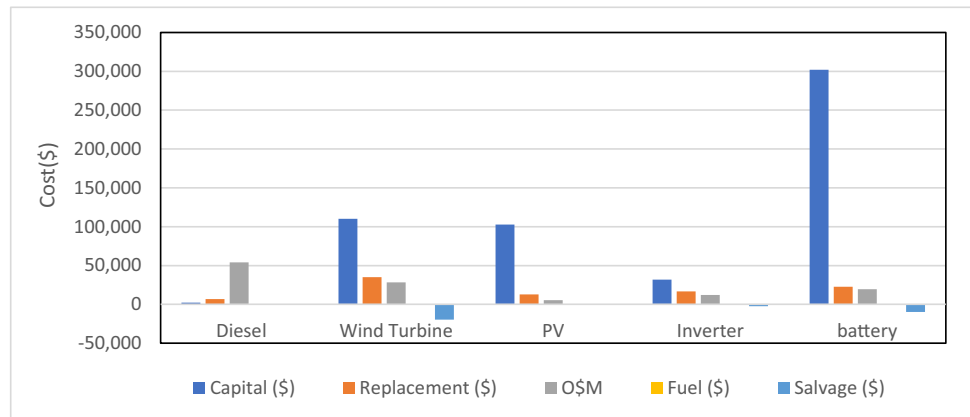


**Fig. 8** Available generation power sources

reliance on the other renewable energy sources, i.e. increasing the PV and wind turbines sizes, resulting in an increase in NPC to \$906,964.1. Finally, the impact of PV derating on the system was evaluated, and the results showed that as the derating value decreased, the installed PV size and NPC both decreased. For example, when the derating values were 80%, 88%, and 95%, the installed PV sizes were \$97.56936, \$85.62402, and \$81.39982, respectively, and the corresponding NPC values were

\$864,664.7, \$853,634.6, and \$843,792.4, respectively. Overall, these findings highlight the importance of considering these key factors when designing and optimizing hybrid renewable energy systems. Tables 15, 16 and 17 show the impact of PV capital cost, diesel fuel price, and PV derating changes on the configurations of the best designed microgrid in the sub-Sect. (4.3). The basic designs, the designs without considering the uncertainty, have been highlighted with blue color in these tables.

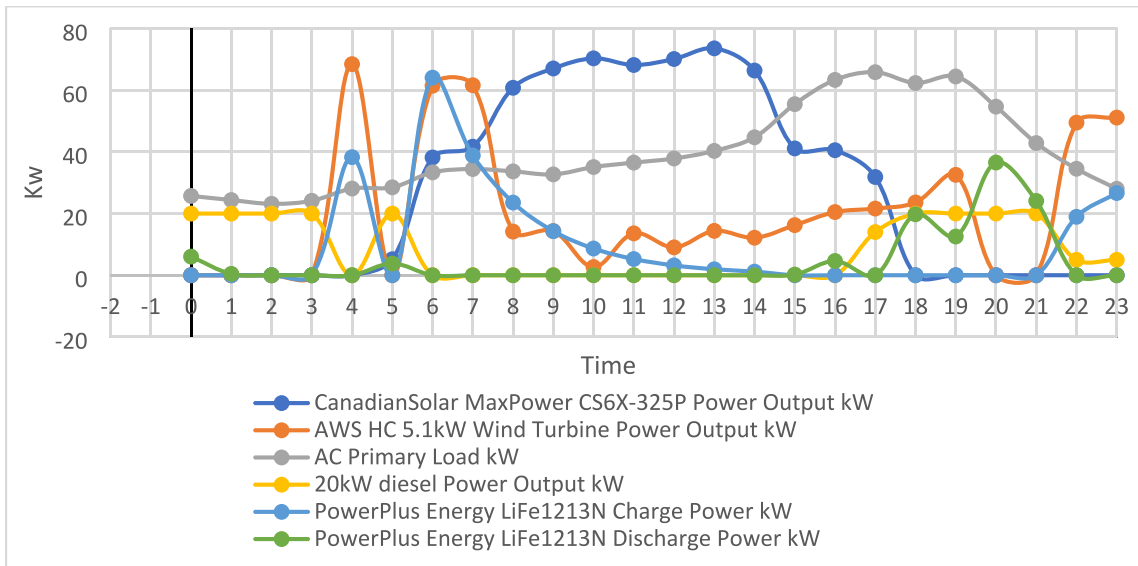


Fig. 9 Daily load demand, along with the power source generation

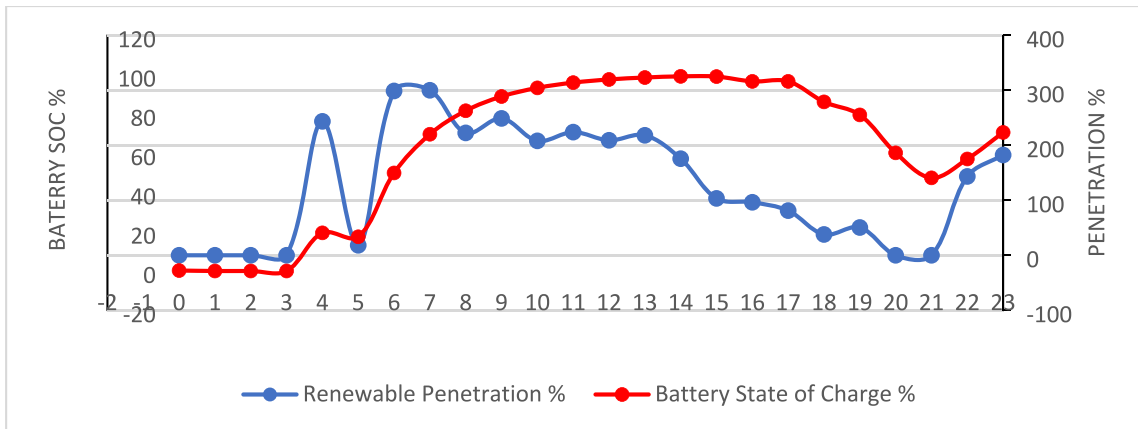


Fig. 10 Renewable energy penetration and the battery state of charge

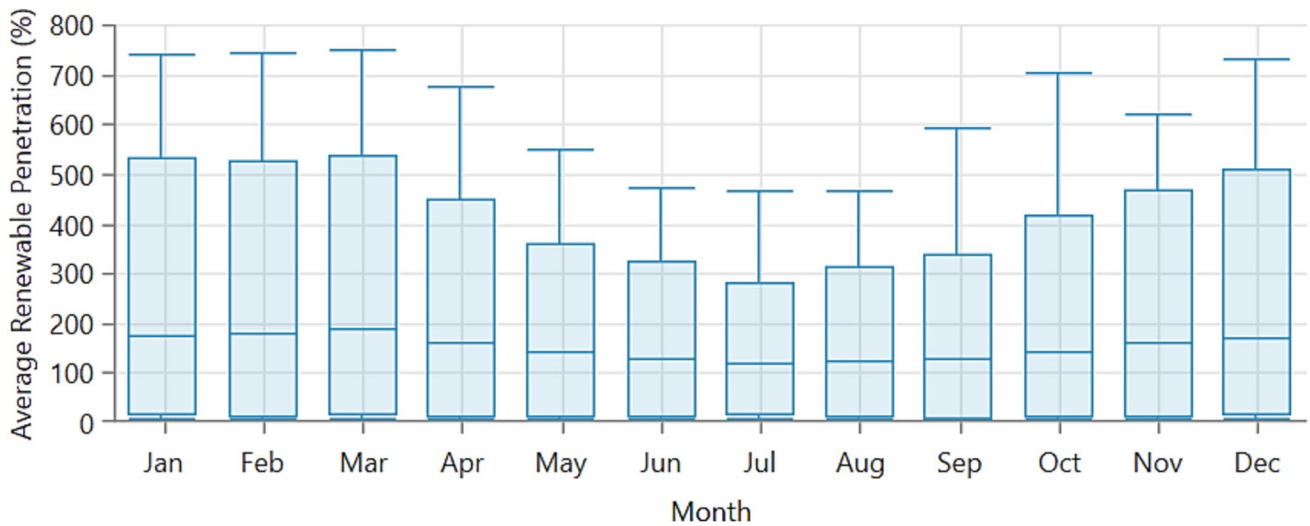


Fig. 11 Renewable penetration monthly averages

**Table 15** Impact of the PV capital cost ratio change on the design of isolated hybrid microgrids

| Design # | PV capital cost ratio (%) | PV (kW)  | Wind turbine (kW) | Diesel (kW) | BESS (kWh) Lead-acid | BESS (kWh) Lithium-ion | Inverter (kW) | Dispatch Strategy | Total NPC (\$) | Energy cost (\$/kWh) | CO <sub>2</sub> (kg/yr.) |
|----------|---------------------------|----------|-------------------|-------------|----------------------|------------------------|---------------|-------------------|----------------|----------------------|--------------------------|
| 1        | 1                         | 85.62402 | 11                | 20          | -----                | 151                    | 63.46         | LF                | 853634.6       | 0.254                | 64018.15                 |
| 2        | 0.9                       | 85.62402 | 11                | 20          | -----                | 151                    | 63.46         | LF                | 843359.6       | 0.0.251              | 64018.15                 |
| 3        | 0.8                       | 91.41    | 11                | 20          | -----                | 149                    | 61.35         | LF                | 833059.4       | 0.248                | 63828.07                 |

**Table 16** Impact of the diesel fuel price change on the design of isolated hybrid microgrids

| Design # | Diesel Fuel Price (\$/L) | PV (kW) | Wind turbine (kW) | Diesel (kW) | BESS (kWh) Lead-acid | BESS (kWh) Lithium-ion | Inverter (kW) | Dispatch Strategy | Total NPC (\$) | Energy cost (\$/kWh) | CO <sub>2</sub> (kg/yr.) |
|----------|--------------------------|---------|-------------------|-------------|----------------------|------------------------|---------------|-------------------|----------------|----------------------|--------------------------|
| 1        | 0.5                      | 85.6    | 11                | 20          | ---                  | 151                    | 63.46         | LF                | 853634.6       | 0.254                | 64018.15                 |
| 2        | 0.6                      | 90.3    | 12                | 20          | ---                  | 147                    | 63.46         | LF                | 879625.9       | 0.262                | 61287.9                  |
| 3        | 0.7                      | 82.1    | 13                | 20          | ---                  | 150                    | 61.35         | LF                | 906964.1       | 0.270                | 59569.59                 |

**Table 17** Impact of the PV derating change on the design of isolated hybrid microgrids

| Design # | PV Derating (%) | PV (kW)  | Wind turbine (kW) | Diesel (kW) | BESS (kWh) Lead-acid | BESS (kWh) Lithium-ion | Inverter (kW) | Dispatch Strategy | Total NPC (\$) | Energy cost (\$/kWh) | CO <sub>2</sub> (kg/yr.) |
|----------|-----------------|----------|-------------------|-------------|----------------------|------------------------|---------------|-------------------|----------------|----------------------|--------------------------|
| 1        | 80              | 97.56936 | 11                | 20          | ---                  | 153                    | 60.54         | LF                | 864664.7       | 0.2581715            | 66003.95                 |
| 2        | 88              | 85.62402 | 11                | 20          | ---                  | 151                    | 63.46         | LF                | 853634.6       | 0.2548907            | 64018.15                 |
| 3        | 95              | 81.39982 | 11                | 20          | ---                  | 150                    | 61.35         | LF                | 843792.4       | 0.251951             | 63828.07                 |

## Conclusion and Policy Implications

This study presents an optimal design framework for an isolated microgrid for a remote area in Egypt with desert climate. Specifically, it focuses on a small Nubian village comprising ten houses located in the new Nubian city of Wadi Karkar within the Aswan governorate, serving as a case study. The residential load curves have been created for 12 months. The design has been carried out aiming for minimizing the total net present cost (NPC), the Cost of Energy (COE), and the greenhouse gas emissions. Renewable energy resources (RES) were selected based on site-measured data, and the system design has been optimized using the HOMER software. A hybrid solar PV, wind turbine, diesel, and battery energy system was implemented, and the optimal mechanical tracking system and best design based on battery technologies have been selected. The research indicated that the optimal system design for the given loads in the understudy Nubian village includes an 85.62 kW PV array, a 20 kW diesel engine, 11 wind turbines with 5.1 output power each, 151 Li-on batteries, and a converter with a power rating of 63.4 kW, resulting in achieving an acceptable environmental gas emissions of 64018.15 kg/yr., total NPC of \$ 853634.6, and COE of \$ 0.255. Utilizing deferrable loads, like a water pumping system, is used in this paper which presents a hopeful approach to handle excess electrical energy in isolated microgrids. This study conducted a sensitivity analysis to demonstrate the impact of PV capital cost, diesel fuel price, and PV derating on the performance and economics of a hybrid renewable energy system. The findings underscore the importance of considering these factors during the design and optimization of such systems. Further, a 7 years payback of a 25-years-lifetime isolated hybrid microgrid has been achieved. This optimal design supports the claim that, for applications with no prospect of grid connection, a hybrid system is a less expensive and more environmentally friendly alternative than a standalone diesel generator.

**Nomenclature** SOC: State Of Charge; REF: Renewable Energy Fraction; NPC: Net Present Cost; COE: Cost of Energy; RES: Renewable Energy Resources; MGs: Microgrids; CC: Cycle Charging dispatch control strategies; LF: Load Following dispatch control strategies; PV: Photovoltaic; HES: Hybrid Energy Systems; CO<sub>2</sub>: Carbon Dioxide; IPCC: Intergovernmental Panel on Climate Change; AC/DC: Alternating/Direct Current; BESS: Battery Energy Storage System; GHG: Greenhouse Gas; IRR: Internal Rate of Return; ROI: Return on Investment; VA cont.: Vertical-Axis continuous tracking; HA cont.: Horizontal-axis continuous tracking; 2A cont.: Dual-axis continuous tracking; HA daily: Horizontal-axis daily tracking; HA weekly: Horizontal-axis weekly tracking; HA monthly: Horizontal-axis monthly tracking

**Acknowledgements** This paper is based upon work supported by the Egyptian Science, Technology & Innovation Funding Authority (STDF) under grant number 44236, and the National Key Research and Development Plan Programs of China, Intergovernmental key projects, China-Egypt, Grant Number: 2022YFE0120700. In addition, the authors would like to thank Control Group Company, Egypt, and Gila Al-Tawakol Electric Company, Egypt for their technical support for this research.

**Data Availability** Data available on request from the authors.

## Declarations

**Conflict of Interest** The authors declare that they have no conflict of interest.

## References

- Pörtner H-O et al (2019) The ocean and cryosphere in a changing climate. In: IPCC special report on the ocean and cryosphere in a changing climate, pp 1155. <https://doi.org/10.1017/9781009157964>
- Olhoff A, Christensen JM (2020) Emissions gap report 2020
- Faragalla A, Abdel-Rahim O, Orabi M, Abdelhameed EH (2022) Enhanced Virtual Inertia Control for Microgrids with High-Penetration Renewables Based on Whale Optimization. *Energies* 15(23):9254
- Friedlingstein P et al (2019) Global carbon budget 2019. *Earth Syst Sci Data* 11(4):1783–1838
- Wang D, Grimmelt M (2023) Climate influence on the optimal stand-alone microgrid system with hybrid storage—A comparative study. *Renew Energy* 208:657–664
- Change, Projected Climate (2018) Global warming of 1.5° C. World Meteorological Organization, Geneva
- Kiehadrouinezhad M, Merabet A, Abo-Khalil AG, Salameh T, Ghenai C (2022) Intelligent and Optimized Microgrids for Future Supply Power from Renewable Energy Resources: A Review. *Energies* 15(9):3359
- Kumar NM, Chopra SS, Chand AA, Elavarasan RM, Shafiullah G (2020) Hybrid renewable energy microgrid for a residential community: A techno-economic and environmental perspective in the context of the SDG7. *Sustainability* 12(10):3944
- Rangu SK, Lolla PR, Dhenuvakonda KR, Singh AR (2020) Recent trends in power management strategies for optimal operation of distributed energy resources in microgrids: A comprehensive review. *Int J Energy Res* 44(13):9889–9911
- Vergine S, Álvarez-Arroyo C, D'Amico G, Escaño JM, Alvarado-Barrios L (2022) Optimal management of a hybrid and isolated microgrid in a random setting. *Energy Rep* 8:9402–9419
- Ribó-Pérez D, Herraiz-Cañete Á, Alfonso-Solar D, Vargas-Salgado C, Gómez-Navarro T (2021) Modelling biomass gasifiers in hybrid renewable energy microgrids; a complete procedure for enabling gasifiers simulation in HOMER. *Renewable Energy* 174:501–512
- Kamal MM, Ashraf I, Fernandez E (2023) Optimal sizing of standalone rural microgrid for sustainable electrification with renewable energy resources. *Sustain Cities Soc* 88:104298
- Kizito R, Li X, Sun K, Li S (2020) Optimal distributed generator placement in utility-based microgrids during a large-scale grid disturbance. *IEEE Access* 8:21333–21344
- Roslan M, Hannan M, Ker PJ, Uddin M (2019) Microgrid control methods toward achieving sustainable energy management. *Appl Energy* 240:583–607
- Clairand J-M, Serrano-Guerrero X, González-Zumba A, Escrivá-Escrivá G (2022) Techno-Economic Assessment of Renewable Energy-based Microgrids in the Amazon Remote Communities in Ecuador. *Energy Technol* 10(2):2100746
- Umar A, Kumar D, Ghose T (2022) Blockchain-based decentralized energy intra-trading with battery storage flexibility in a community microgrid system. *Appl Energy* 322:119544
- Khorasany M, Azuatalam D, Glasgow R, Liebman A, Razzaghi R (2020) Transactive energy market for energy management in microgrids: The monash microgrid case study. *Energies* 13(8):2010

18. Tomin N et al (2022) Design and optimal energy management of community microgrids with flexible renewable energy sources. *Renew Energy* 183:903–921
19. Canales FA, Jadwiszczak P, Jurasz J, Wdowikowski M, Ciapała B, Kaźmierczak B (2020) The impact of long-term changes in air temperature on renewable energy in Poland. *Sci Total Environ* 729:138965
20. Peter J (2019) How does climate change affect electricity system planning and optimal allocation of variable renewable energy? *Appl Energy* 252:113397
21. Konneh KV et al (2021) Optimal design and performance analysis of a hybrid off-grid renewable power system considering different component scheduling, PV modules, and solar tracking systems. *IEEE Access* 9:64393–64413
22. Chedid R, Sawwas A, Fares D (2020) Optimal design of a university campus micro-grid operating under unreliable grid considering PV and battery storage. *Energy* 200:117510
23. Helal A, El-Mohr R, Eldosouki H (2012) Optimal design of hybrid renewable energy system for electrification of a remote village in Egypt. *CCCA12*. IEEE
24. Abo-Zahhad EM et al (2024) Evaluation of solar PV-based microgrids viability utilizing single and multi-criteria decision analysis. *Renew Energy* 221:119713
25. Tran QT, Davies K, Sepasi S (2021) Isolation Microgrid Design for Remote Areas with the Integration of Renewable Energy: A Case Study of Con Dao Island in Vietnam. *Clean Technol* 3(4):804–820
26. Ozogbuda J, Iqbal MT (2021) Design of a DC Microgrid System for a Remote Community in Nigeria. *Eur J Electr Eng Comput Sci* 5(6):29–35
27. Kebede AA et al (2021) Techno-economic analysis of lithium-ion and lead-acid batteries in stationary energy storage application. *J Energy Storage* 40:102748
28. Li B, Roche R, Miraoui A (2017) Microgrid sizing with combined evolutionary algorithm and MILP unit commitment. *Appl Energy* 188:547–562
29. Yasin A (2019) Energy management of a stand-alone DC microgrid based on PV/Wind/Battery/Diesel Gen. combined with supercapacitor. *Int J Renew Energy Res (IJRER)* 9(4):1811–1826
30. Mansouri SA, Ahmarinejad A, Nematbakhsh E, Javadi MS, Nezhad AE, Catalão JP (2022) A sustainable framework for multi-microgrids energy management in automated distribution network by considering smart homes and high penetration of renewable energy resources. *Energy* 245:123228
31. Mansouri SA, Ahmarinejad A, Nematbakhsh E, Javadi MS, Jordehi AR, Catalao JP (2021) Energy management in microgrids including smart homes: A multi-objective approach. *Sustain Cities Soc* 69:102852
32. Mishra S, Saini G, Saha S, Chauhan A, Kumar A, Maity S (2022) A survey on multi-criterion decision parameters, integration layout, storage technologies, sizing methodologies and control strategies for integrated renewable energy system. *Sustain Energy Technol Assess* 52:102246
33. Zhou A, Yan R, Saha TK (2019) Capacity and control strategy design of isolated micro-grid with high renewable penetration. *IEEE Trans Sustain Energy* 11(3):1173–1184
34. Javed MS, Song A, Ma T (2019) Techno-economic assessment of a stand-alone hybrid solar-wind-battery system for a remote island using genetic algorithm. *Energy* 176:704–717
35. Singh P, Pandit M, Srivastava L (2022) Techno-socio-economic-environmental estimation of hybrid renewable energy system using two-phase swarm-evolutionary algorithm. *Sustain Energy Technol Assess* 53:102483
36. Jain S, Sawle Y (2021) Optimization and Comparative Economic Analysis of Standalone and Grid-Connected Hybrid Renewable Energy System for Remote Location. *Front. Front Energy Res* 9:724162
37. Aziz AS, Tajuddin MFN, Adzman MR, Ramli MA, Mekhilef S (2019) Energy management and optimization of a PV/diesel/battery hybrid energy system using a combined dispatch strategy. *Sustainability* 11(3):683
38. Conteh F et al (2023) Long-term forecast of sierra leone's energy supply and demand (2019–2040): a LEAP model application for sustainable power generation system. *Sustainability* 15(15):11838

**Publisher's Note** Springer Nature remains neutral with regard to jurisdictional claims in published maps and institutional affiliations.

Springer Nature or its licensor (e.g. a society or other partner) holds exclusive rights to this article under a publishing agreement with the author(s) or other rightsholder(s); author self-archiving of the accepted manuscript version of this article is solely governed by the terms of such publishing agreement and applicable law.